Coordination Networks of 3,3′-Dicyanodiphenylacetylene and Silver(I) Salts: Structural Diversity through Changes in Ligand Conformation and Counterion

Keith A. Hirsch,[†] Scott R. Wilson,[†] and Jeffrey S. Moore*[,‡]

Departments of Chemistry and Materials Science and Engineering, The University of Illinois at Urbana-Champaign, 600 S. Mathews Avenue, Urbana, Illinois 61801

Received February 7, 1997[⊗]

Coordination networks of 3,3′-dicyanodiphenylacetylene (3,3′-DCPA, **1**) with silver(I) salts characterized by single-crystal X-ray analysis are described. Network topology is found to depend on both the counterion and solvent employed during crystallization. The conformation adopted by the ligand varies between planar *cisoid* and planar *transoid*. With silver(I) triflate ($AgCF_3SO_3$) in benzene, a sheet structure of composition $[Ag(\mathbf{1})CF_3SO_3]C_6H_6$ (**2**) forms in which silver(I) is five-coordinate and bonds to two nitrogen atoms of distinct 3,3′-DCPA molecules, another silver(I) ion, and two oxygen atoms of the triflate ions. Changing the solvent to toluene produces an undulating sheet structure of composition $[Ag_2(\mathbf{1})(CF_3SO_3)_2]$ (**3**) in which silver(I) is six-coordinate, bonding to a ligand nitrogen atom, to four oxygen atoms of bridging triflate ions, and to a neighboring silver(I) ion. In both triflate structures, 3,3′-DCPA adopts a *transoid* conformation with respect to the positioning of the nitrile groups. With silver(I) hexafluorophosphate ($AgPF_6$), silver(I) hexafluoroarsenate ($AgAsF_6$), or silver(I) hexafluoroantimonate ($AgSbF_6$), 2-fold interpenetrated sheet structures $[Ag(\mathbf{1})_2]XF_6$ (X = P (**4**), As (**5**), or Sb (**6**)) are obtained in which 3,3′-DCPA coordinates to tetrahedral silver(I) ions in a *cisoid* conformation. In spite of the large difference in counterion size, minimal network deformation is observed among these systems. Interestingly, with silver(I) perchlorate hydrate ($AgClO_4 \cdot xH_2O$, $x \sim 1$), 3,3′-DCPA coordinates in a *transoid* conformation to tetrahedral silver(I) ions to form the 8-fold interpenetrated diamondoid network $[Ag(\mathbf{1})_2]ClO_4 \cdot H_2O$ (**7**). An analysis of the packing of these networks is provided, and the results are compared to complementary systems previously reported from our study of coordination networks of dinitriles and silver(I) salts.

Introduction

Interest in coordination networks formed from polyfunctional organic ligands and transition metal salts has been driven by the belief that novel materials may be "engineered" by the use of ligands of well-defined topicity.[1] However, the rational design of these materials is complicated by the uncertain coordination propensity of the metal ion which is influenced by such factors as the counterion, solvent, and the ligand geometry. Thus, understanding how these considerations affect metal coordination and influence crystal packing is at the heart of controlling coordination network assembly. Further, it is felt that the ability to predict topology of coordination networks relies on analysis of many structures in order for trends to be discovered. In an attempt to address this issue, we previously reported the role played by the counterion in coordination networks of silver(I) salts with the conformationally rigid ligands

Chart 1. *Transoid* and *Cisoid* Conformations of 3,3′-Dicyanodiphenylacetylene (3,3′-DCPA, **1**)

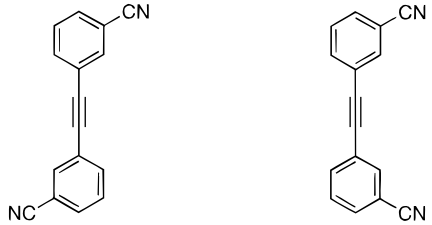

A **B**

4,4′-biphenyldicarbonitrile[2] and 4,4′-dicyanodiphenylacetylene.[3] We have now extended this study to 3,3′-dicyanodiphenylacetylene (3,3′-DCPA, **1**), a ditopic ligand which may be viewed as an off-axis rigid rod in the *transoid* conformation or a kinked ligand in the *cisoid* conformation (**A** and **B**, respectively, in Chart 1).

Here we report X-ray crystal structures of 3,3′-DCPA with silver(I) triflate ($AgCF_3SO_3$), silver(I) hexafluorophosphate ($AgPF_6$), silver(I) hexafluoroarsenate ($AgAsF_6$), silver(I) hexafluoroantimonate ($AgSbF_6$), and silver(I) perchlorate hydrate ($AgClO_4 \cdot xH_2O$, $x \sim 1$). The topology of the ensuing coordination networks is found to depend strongly on the counterion and whether the ligand adopts a *transoid* or *cisoid* conformation. Included is an analysis of the packing of the networks, and comparisons are made to structures we have previously reported.[2,3] From this study, some general trends and concepts are illustrated for the packing of coordination networks.

* To whom correspondence should be addressed.
[†] Department of Chemistry, The University of Illinois at Urbana-Champaign.
[‡] Departments of Chemistry and Materials Science and Engineering, The University of Illinois at Urbana-Champaign.
[⊗] Abstract published in *Advance ACS Abstracts,* June 1, 1997.

(1) (a) Robson, R.; Abrahams, B. F.; Batten, S. R.; Gable, R. W.; Hoskins, B. F.; Liu, J. In *Supramolecular Architecture*; Bein, T., Ed.; American Chemical Society: Washington, DC, 1992; p 256. (b) Fujita, M.; Kwon, Y. J.; Washizu, S.; Ogura, K. *J. Am. Chem. Soc.* **1994**, *116*, 1151. (c) Gardner, G. B.; Venkataraman, D.; Moore, J. S.; Lee, S. *Nature* **1995**, *374*, 792. (d) Venkataraman, D.; Gardner, G. B.; Lee, S.; Moore, J. S. *J. Am. Chem. Soc.* **1995**, *117*, 11600. (e) Yaghi, O. M.; Li, G.; Li, H. *Nature* **1995**, *378*, 703.
(2) (a) Hirsch, K. A.; Venkataraman, D.; Wilson, S. R.; Moore, J. S.; Lee, S. *J. Chem. Soc., Chem. Commun.* **1995**, 2199. (b) Venkataraman, D.; Lee, S.; Moore, J. S.; Zhang, P.; Hirsch, K. A.; Gardner, G. B.; Covey, A. C.; Prentice, C. L. *Chem. Mater.* **1996**, *8*, 2030. (c) Hirsch, K. A.; Wilson, S. R.; Moore, J. S. *Chem. Eur. J.* **1997**, *3*, 765.
(3) Hirsch, K. A.; Wilson, S. R.; Moore, J. S. *Acta Crystallogr.* **1996**, *C52*, 2419.

S0020-1669(97)00150-X CCC: $14.00

Experimental Section

General Methods. Unless otherwise indicated, all starting materials were obtained from commercial suppliers (Aldrich, J. T. Baker, Eastman, EM Science, Fischer, Johnson-Matthey, Lancaster, and Mallinckrodt) and were used without further purification. Dichloromethane, ethyl acetate, and hexane were distilled prior to use. (Trimethylsilyl)acetylene (Farchan) was dried over anhydrous $MgSO_4$ and collected *via* vacuum transfer prior to use. Silver(I) triflate, silver(I) hexafluorophosphate, silver(I) hexafluoroarsenate (Alfa), and silver(I) hexafluoroantimonate were stored in a desiccator with Drierite as the drying agent. Silver(I) perchlorate hydrate was stored in a refrigerator at 3 °C. All atmosphere-sensitive reactions were conducted under nitrogen using a Schlenk vacuum line. No precautions were taken to exclude water or air during crystallizations. Analytical thin-layer chromatography (TLC) was performed on KIESELGEL F-254 precoated silica gel plates. Visualization was accomplished with a UV light. Flash chromatography was carried out with Silica Gel 60 (230−400 mesh) from EM Science.

^{1}H and ^{13}C NMR spectra were recorded on a Varian Unity 400 spectrometer. Chemical shifts were recorded in parts per million (δ), and splitting patterns were designated as s, singlet, or m, multiplet. Chloroform (δ 7.26 for ^{1}H, δ 77.0 for ^{13}C) was used as an internal standard for chloroform-*d*. Gas chromatography (GC) was performed on a Hewlett-Packard HP-5890 Series II gas chromatograph equipped with a 12.5 m × 0.2 m × 0.5 μm HP-1 methyl silicone column and fitted with a flame ionization detector using helium carrier gas at 30 mL/min. Low-resolution electron impact mass spectra were obtained using a Hewlett-Packard 5890 gas chromatograph combined with a 5970 Series mass selective detector equipped with a 30 m HP-1 capillary column operating at 70 eV. High-resolution mass spectra were obtained on a Finnigan-MAT 731 spectrometer operating at 70 eV. Elemental analyses were performed by the University of Illinois Microanalytical Service Laboratory by combustion analysis on a Leeman Labs, Inc., Model CE440 elemental analyzer. The infrared spectrum of **8** was recorded on an IBM IR/32 FTIR spectrometer, and absorbances are reported in cm^{-1}.

Crystallization with silver(I) triflate was accomplished by heating and slow cooling in a programmable oven equipped with a Thermolyne temperature controller. Otherwise, crystallization conditions were optimized for each complex and detailed procedures are provided below. All crystals were stored in the dark until the collection of X-ray data. For X-ray analysis, all crystals were mounted using Paratone-N oil (Exxon).

X-ray data were collected on a Siemens SMART system equipped with a CCD detector at −75 °C using Mo Kα (λ = 0.710 73 Å) as the incident radiation. The intensity data were reduced by profile analysis and corrected for Lorentz, polarization, and absorption effects. Cell parameters and atomic coordinates were tested for higher symmetry using the PLATON program.[4] Structure solutions were obtained by direct methods and were refined using full-matrix least-squares on all reflections, based on F_o^2, with SHELXTL.[5]

Caution! *One of the crystallization procedures involves $AgClO_4 \cdot H_2O$, which is an oxidizer.*

3-((Trimethylsilyl)ethynyl)benzonitrile (8). 3-Bromobenzonitrile (12.02 g, 66.01 mmol), $Pd(dba)_2$ (0.76 g, 1.32 mmol), CuI (0.25 g, 1.33 mmol), and Ph_3P (1.73 g, 6.59 mmol) were combined with triethylamine (170 mL) in a dry, heavy-walled tube sealed with a Teflon screw cap. The resulting mixture was degassed and back-filled with nitrogen three times and left under nitrogen at room temperature. Dry (trimethylsilyl)acetylene (14.0 mL, 99.06 mmol) was then added *via* syringe. The tube was then sealed with the Teflon screw cap and placed in an oil bath. Heating at 74 °C for 21 h produced an orange solution with a precipitate which was presumed to be triethylammonium bromide. The mixture was cooled to room temperature, diluted with Et_2O (1 L), and filtered to remove the precipitate. The yellow filtrate was concentrated *in vacuo* to yield crude product as a dark red liquid. Column chromatography (18/1 hexane/ethyl acetate) afforded **8** as a light yellow oil which crystallized as a white solid upon standing under vacuum for 1 h (12.18 g, 93% yield, 99% pure by GC): R_f 0.32 (18/1 hexane/ethyl acetate); ^{1}H NMR (400 MHz, $CDCl_3$) δ 7.72 (m, 1H), 7.65 (m, 1H), 7.57 (m, 1H), 7.40 (m, 1H), 0.25 (s, 9H); ^{13}C NMR (100 MHz, $CDCl_3$) δ 135.9, 135.2, 131.5, 129.1, 124.6, 117.9, 112.6, 102.2, 97.3, −0.3; IR (neat) 3071, 2959, 2899, 2234, 2153 cm^{-1}; LRMS (EI) *m*/*e* 199 (19), 184 (100); HRMS (EI) calcd for $C_{12}H_{13}NSi^+$ 199.0817, found 199.0817. Anal. Calcd for $C_{12}H_{13}NSi$: C, 72.31; H, 6.57; N, 7.03. Found: C, 72.54; H, 6.77; N, 7.23.

3,3′-Dicyanodiphenylacetylene (1). To a solution of trimethylsilyl-protected acetylene **8** (3.83 g, 19.22 mmol) in CH_2Cl_2 (10 mL) and MeOH (20 mL) was added a trace of K_2CO_3. The yellow mixture was degassed and back-filled with nitrogen three times and stirred under nitrogen at room temperature for 50 min. The conversion of **8** to 3-ethynylbenzonitrile was confirmed by GC and GC/MS (LRMS (EI) showed the desired molecular ion of *m*/*e* 127 for $C_9H_5N^+$). The terminal acetylene was not isolated due to its volatility. Next, in a dry, heavy-walled tube sealed with a Teflon screw cap, was placed 3-bromobenzonitrile (3.86 g, 21.19 mmol), $Pd(dba)_2$ (0.22 g, 0.39 mmol), CuI (0.08 g, 0.40 mmol), Ph_3P (0.51 g, 1.93 mmol), and triethylamine (50 mL). This mixture was degassed and back-filled with nitrogen three times and left under nitrogen at room temperature. The CH_2Cl_2/MeOH solution of 3-ethynylbenzonitrile was then added *via* syringe. The tube was sealed with the Teflon screw cap and placed in an oil bath. Heating at 72 °C for 22 h produced a brown solution with a precipitate which was presumed to be triethylammonium bromide. This mixture was cooled to room temperature, dissolved in CH_2Cl_2 (200 mL), and concentrated *in vacuo* to yield crude product as a brown solid. Column chromatography (CH_2Cl_2) afforded **1** as a light yellow solid (3.33 g, 76% yield, 98% pure by GC). An analytically pure sample (elemental analysis) was prepared by recrystallization from 1/1 benzene/hexane to yield a white solid: R_f 0.42 (CH_2Cl_2); ^{1}H NMR (400 MHz, $CDCl_3$) δ 7.81 (m, 2H), 7.75 (m, 2H), 7.65 (m, 2H), 7.50 (m, 2H); ^{13}C NMR (100 MHz, $CDCl_3$) δ 135.7, 134.9, 132.0, 129.4, 123.8, 117.8, 113.0, 89.0; LRMS (EI) *m*/*e* 229 (17), 228 (100), 227 (10), 201 (10); HRMS (EI) calcd for $C_{16}H_8N_2^+$ 228.0687, found 228.0685. Anal. Calcd for $C_{16}H_8N_2$: C, 84.19; H, 3.53; N, 12.28. Found: C, 84.17; H, 3.36; N, 12.37.

[Ag(3,3′-dicyanodiphenylacetylene)CF_3SO_3]C_6H_6 (2). A mixture of 3,3′-dicyanodiphenylacetylene (10 mg, 0.04 mmol) and silver(I) triflate (12 mg, 0.05 mmol) in benzene (5 mL) was prepared in a clean vial with a Teflon-lined screw cap and heated in a programmable oven. Heating from room temperature to 100 °C at 20 °C/h, holding at 100 °C for 2 h, and cooling to room temperature at 1.2 °C/h yielded X-ray-quality material as colorless columnar crystals. Anal. Calcd for $C_{23}H_{14}N_2O_3F_3SAg$: C, 49.04; H, 2.51; N, 4.97. Found: C, 48.80; H, 2.45; N, 4.97.

[Ag_2(3,3′-dicyanodiphenylacetylene)(CF_3SO_3)$_2$] (3). A mixture of 3,3′-dicyanodiphenylacetylene (10 mg, 0.04 mmol) and silver(I) triflate (12 mg, 0.05 mmol) in toluene (5 mL) was prepared in a clean vial with a Teflon-lined screw cap and heated in a programmable oven. Heating from room temperature to 100 °C at 20 °C/h, holding at 100 °C for 2 h, and cooling to room temperature at 1.2 °C/h yielded a homogeneous solution. Allowing the vial to stand for 7 d at room temperature afforded material suitable for X-ray analysis as colorless prisms. Anal. Calcd for $C_{18}H_8N_2O_6F_6S_2Ag_2$: C, 29.13; H, 1.09; N, 3.77. Found: C, 29.13; H, 1.16; N, 3.81.

[Ag(3,3′-dicyanodiphenylacetylene)$_2$]PF_6 (4). A mixture of 3,3′-dicyanodiphenylacetylene (10 mg, 0.04 mmol) and silver(I) hexafluorophosphate (12 mg, 0.05 mmol) in ethanol (5 mL) was prepared in a clean vial with a Teflon-lined screw cap and heated in an oil bath. After 70 min, a homogeneous solution was observed at 70 °C. The solution was cooled to room temperature overnight, and no crystals or precipitates were observed. However, evaporation of ethanol by slightly loosening the screw cap produced colorless prisms after 8 d for which an X-ray data set was collected. Anal. Calcd for $C_{32}H_{16}N_4F_6PAg$: C, 54.18; H, 2.27; N, 7.90. Found: C, 53.72; H, 2.00; N, 7.90.

[Ag(3,3′-dicyanodiphenylacetylene)$_2$]AsF_6 (5). A mixture of 3,3′-dicyanodiphenylacetylene (10 mg, 0.04 mmol) and silver(I) hexafluoroarsenate (14 mg, 0.05 mmol) in ethanol (5 mL) was prepared in a clean vial with a Teflon-lined screw cap and heated in an oil bath. A homogeneous solution was obtained by heating to 70 °C for 15 h.

(4) Spek, A. L. *J. Appl. Crystallogr.* **1988**, *21*, 578.

(5) The SHELXTL X-ray structure refinement package consists of SAINT Version 4, SHELXTL Version 5, and SMART Version 4 and is marketed by Siemens Industrial Automation, Inc., Madison, WI.

Scheme 1. Synthesis of 3,3′-DCPA (**1**)[a]

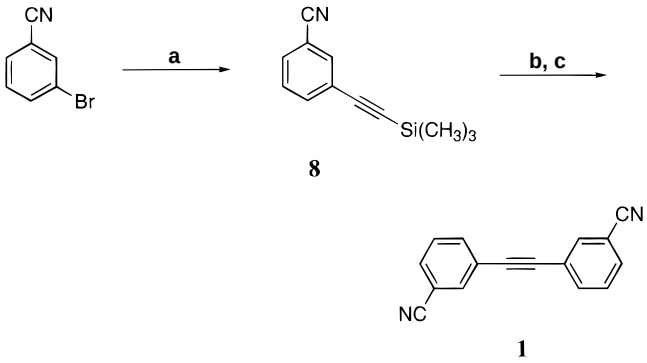

[a] (a) (trimethylsilyl)acetylene, $Pd(dba)_2$, CuI, Ph_3P, Et_3N, N_2, 74 °C, 21 h, 93%; (b) K_2CO_3, MeOH, CH_2Cl_2, N_2, rt, 50 min; (c) 3-bromobenzonitrile, $Pd(dba)_2$, CuI, Ph_3P, Et_3N, N_2, 72 °C, 22 h, 76% (two steps).

Cooling the solution overnight to room temperature yielded no crystals or precipitates. Crystals suitable for X-ray analysis were obtained as colorless prisms by evaporation of ethanol over 4 d by slightly loosening the screw cap. Anal. Calcd for $C_{32}H_{16}N_4F_6AsAg$: C, 48.94; H, 2.05; N, 7.13. Found: C, 50.60; H, 2.20; N, 7.40.

[Ag(3,3′-dicyanodiphenylacetylene)$_2$]SbF_6 (6). A mixture of 3,3′-dicyanodiphenylacetylene (10 mg, 0.04 mmol) and silver(I) hexafluoroantimonate (17 mg, 0.05 mmol) in ethanol (5 mL) was prepared in a clean vial with a Teflon-lined screw cap and heated in an oil bath. After 1 h, a homogeneous solution was obtained at 78 °C. As with complexes **4** and **5**, cooling to room temperature overnight yielded no crystals or precipitates. Evaporation of ethanol over 16 d by slightly loosening the screw cap yielded material suitable for X-ray analysis as colorless columnar crystals. Anal. Calcd for $C_{32}H_{16}N_4F_6AgSb$: C, 46.19; H, 1.94; N, 6.73. Found: C, 47.29; H, 2.09; N, 6.55.

[Ag(3,3′-dicyanodiphenylacetylene)$_2$]ClO_4·H_2O (7). A solution of 3,3′-dicyanodiphenylacetylene (10 mg, 0.04 mmol) and silver(I) perchlorate hydrate ($AgClO_4$·xH_2O, $x \sim 1$; 10 mg, 0.05 mmol) in acetone (8 mL) was prepared in a clean vial with a screw cap. Evaporation of acetone over 5 d by slightly loosening the screw cap yielded both thin, colorless needles and tabular crystals. The needles were found to diffract too weakly for X-ray analysis; however, a tabular crystal diffracted suitably and was characterized as complex **7**.

Results and Discussion

Synthesis of 3,3′-Dicyanodiphenylacetylene (3,3′-DCPA, 1). 3,3′-DCPA was chosen as a simple yet interesting dinitrile to study due to its presumed conformational flexibility. The possibility for the ligand to adopt either a *transoid* or *cisoid* conformation potentially allows access to networks of novel topology. It was also felt that this inherent flexibility could impart good solubility of 3,3′-DCPA in common organic solvents. Relatively poor solubility was encountered in our previous work with 4,4′-dicyanodiphenylacetylene,[3] which made crystallization with silver(I) salts rather difficult.

3,3′-DCPA was synthesized *via* the straightforward three-step procedure shown in Scheme 1. Palladium-catalyzed cross coupling[6] of (trimethylsilyl)acetylene with commercially available 3-bromobenzonitrile produced the trimethylsilyl-protected 3-ethynylbenzonitrile (**8**) in high yield. Subsequent deprotection to the terminal acetylene was achieved with a trace of K_2CO_3 in a solution of MeOH and CH_2Cl_2. Due to the volatility of the terminal acetylene, this material was not isolated. 3,3′-DCPA was next prepared in good yield by palladium-catalyzed cross coupling of the terminal acetylene with 3-bromobenzonitrile.

Crystallization of 3,3′-DCPA with Silver(I) Salts. The adequate solubility of 3,3′-DCPA in common organic solvents made crystallization with silver(I) salts relatively straightforward. With $AgCF_3SO_3$, heating and slow cooling in either benzene or toluene provided suitable crystals for X-ray analysis. In fact, these two solvents yielded different structures which are described below. With $AgPF_6$, $AgAsF_6$, or $AgSbF_6$, heating and slow cooling in absolute ethanol followed by slow evaporation of the solvent yielded single crystals suitable for X-ray structure determination. With $AgClO_4$·H_2O, crystallization was performed by slow evaporation at room temperature in acetone. This procedure produced two different crystalline habits—thin needles and tabular crystals. The needles were found to diffract very weakly, and the structure of this material could not be determined. However, the tabular crystals did diffract well and a discussion of the resulting structure is provided below. Crystallization with $AgBF_4$ in ethanol by heating and slow cooling followed by slow evaporation of the solvent yielded crystals which were not suitable for X-ray analysis. Relevant X-ray data for all of the coordination networks characterized are provided in Table 1.

Crystal Structure of 3,3′-DCPA (1) with $AgCF_3SO_3$ from Benzene: [Ag(1)CF_3SO_3]C_6H_6 (2). Crystallization of 3,3′-DCPA with $AgCF_3SO_3$ in benzene yields the infinite sheet structure **2** in which strands of the organic ligand coordinated to silver(I) ions are bridged by triflate ions (see Figure 1). The metal−ligand stoichiometry is 1:1. In this structure, the 3,3′-DCPA molecules adopt a *transoid* conformation. Surprisingly, the silver(I) ion is five-coordinate[7,8] with a distorted square pyramidal geometry realized by bonding to two ligand nitrogen atoms, two oxygen atoms of triflate ions, and a neighboring silver(I) ion (Figure 1). The Ag···Ag separation[9] is 3.377(1) Å, which is below the sum of the van der Waals radii for silver(I) of 3.40 Å. A long Ag−O interaction distance of 2.573(3) Å is noted *trans* to the Ag···Ag contact, and a shorter Ag−O bond of 2.464(3) Å occupies the apical position.

The infinite sheet topology is formed *via* the bridging of triflate ions as the Ag···Ag interactions simply join two strands to form a finite pair (Figure 1). Along a strand, the C−N−Ag bond angles are nearly linear (166.3(3) and 172.3(3)°) and the Ag−**1**−Ag distance is 17.01 Å. Neighboring strands do not overlap in registry which might be expected in order to maximize $\pi-\pi$ stacking interactions between 3,3′-DCPA molecules. Rather, steric bulk of the triflate ions prevents this

(6) For earlier examples of palladium-catalyzed cross coupling reactions utilized to prepare phenylacetylenes, see: (a) Wu, Z.; Moore, J. S. *Angew. Chem., Int. Ed. Engl.* **1996**, *35*, 297. (b) Zhang, J.; Pesak, D. J.; Ludwick, J. L.; Moore, J. S. *J. Am. Chem. Soc.* **1994**, *116*, 4227. (c) Xu, Z.; Moore, J. S. *Angew. Chem., Int. Ed. Engl.* **1993**, *32*, 1354.

(7) We have performed a comprehensive search of the Cambridge Structural Database in order to tabulate the coordination propensities of transition metals in their various oxidation states. This study indicates, *quantitatively and with statistical reliability*, that silver(I) most often adopts linear, trigonal planar, and tetrahedral coordination geometries. See: Venkataraman, D.; Du, Y.; Wilson, S. R.; Hirsch, K. A.; Zhang, P.; Moore, J. S. *J. Chem. Educ.*, in press. The results of this study are also available on the Internet: http://sulfur.scs.uiuc.edu/.

(8) For other examples of five- and six-coordinate silver(I), see: Carlucci, L.; Ciani, G.; Proserpio, D. M.; Sironi, A. *Angew. Chem., Int. Ed. Engl.* **1995**, *34*, 1895.

(9) For other examples of coordination networks displaying Ag···Ag contacts, see: (a) Michaelides, A.; Kiritsis, V.; Skoulika, S.; Aubry, A. *Angew. Chem., Int. Ed. Engl.* **1993**, *32*, 1495. (b) Masciocchi, N.; Moret, M.; Cairati, P.; Sironi, A.; Ardizzoia, G. A.; La Monica, G. *J. Am. Chem. Soc.* **1994**, *116*, 7668. (c) Masciocchi, N.; Moret, M.; Cairati, P.; Sironi, A.; Ardizzoia, G. A.; La Monica, G. *J. Chem. Soc., Dalton Trans.* **1995**, 1671. (d) Robinson, F.; Zaworotko, M. J. *J. Chem. Soc., Chem. Commun.* **1995**, 2413. (e) Yaghi, O. M.; Li, H. *J. Am. Chem. Soc.* **1996**, *118*, 295. It should be noted that ref 9b describes Ag···Ag contacts as long as 3.449(6) Å.

Table 1. Crystallographic Data for Complexes **2**−**7**

	[Ag(**1**)CF_3SO_3]C_6H_6 (**2**)	[Ag_2(**1**)$(CF_3SO_3)_2$] (**3**)	[Ag(**1**)$_2$]PF_6 (**4**)	[Ag(**1**)$_2$]AsF_6 (**5**)	[Ag(**1**)$_2$]SbF_6 (**6**)	[Ag(**1**)$_2$]ClO_4·H_2O (**7**)
formula	$C_{23}H_{14}N_2O_3F_3SAg$	$C_{18}H_8N_2O_6F_6S_2Ag_2$	$C_{32}H_{16}N_4F_6PAg$	$C_{32}H_{16}N_4F_6AsAg$	$C_{32}H_{16}N_4F_6AgSb$	$C_{32}H_{18}N_4O_5ClAg$
fw	563.29	742.12	709.33	753.28	800.11	663.81
cryst system	monoclinic	monoclinic	triclinic	triclinic	triclinic	orthorhombic
space group	*P*2/*c* (No. 13)	*P*2/*n* (No. 13)	$P\bar{1}$ (No. 2)	$P\bar{1}$ (No. 2)	$P\bar{1}$ (No. 2)	*Ccca* (No. 68)
cryst color	colorless	colorless	colorless	colorless	colorless	colorless
unit cell params	$a = 7.556(1)$ Å	$a = 10.430(1)$ Å	$a = 8.2240(3)$ Å	$a = 8.262(1)$ Å	$a = 8.338(3)$ Å	$a = 13.161(1)$ Å
	$b = 17.005(2)$ Å	$b = 4.9331(9)$ Å	$b = 11.9317(9)$ Å	$b = 11.930(1)$ Å	$b = 11.892(4)$ Å	$b = 15.9101(6)$ Å
	$c = 17.803(2)$ Å	$c = 22.375(3)$ Å	$c = 15.007(1)$ Å	$c = 15.091(2)$ Å	$c = 15.223(6)$ Å	$c = 14.579(1)$ Å
	$\alpha = \gamma = 90°$	$\alpha = \gamma = 90°$	$\alpha = 77.691(6)°$	$\alpha = 77.238(0)°$	$\alpha = 77.030(6)°$	$\alpha = \beta = \gamma = 90°$
	$\beta = 101.482(6)°$	$\beta = 96.387(3)°$	$\beta = 86.815(6)°$	$\beta = 85.945(6)°$	$\beta = 85.051(6)°$	
			$\gamma = 86.944(6)°$	$\gamma = 86.559(3)°$	$\gamma = 86.352(6)°$	
T (°C)	−75	−75	−75	−75	−75	−75
V (Å^3)	2241.6(6)	1144.1(3)	1435.2(1)	1445.6(3)	1464.0(9)	3052.7(3)
Z	4	2	2	2	2	4
ρ_{calcd} (g cm^{-3})	1.669	2.154	1.641	1.731	1.815	1.484
λ (Å) (Mo Kα)	0.710 73	0.710 73	0.710 73	0.710 73	0.710 73	0.710 73
μ (cm^{-1})	10.45	19.82	8.27	19.02	16.59	7.94
unweighted	0.0486 ($F_o > 4\sigma$)	0.0230 ($F_o > 4\sigma$)	0.0845 ($F_o > 4\sigma$)	0.0359 ($F_o > 4\sigma$)	0.0529 ($F_o > 4\sigma$)	0.0368 ($F_o > 4\sigma$)
agreement factor ($R1$)[a]	0.1146 (all data)	0.0263 (all data)	0.1657 (all data)	0.0472 (all data)	0.1103 (all data)	0.0575 (all data)
weighted agreement	0.0801 ($F_o > 4\sigma$)	0.0509 ($F_o > 4\sigma$)	0.1094 ($F_o > 4\sigma$)	0.0838 ($F_o > 4\sigma$)	0.0942 ($F_o > 4\sigma$)	0.0799 ($F_o > 4\sigma$)
factor ($wR2$)[b]	0.1043 (all data)	0.0524 (all data)	0.1483 (all data)	0.0937 (all data)	0.1242 (all data)	0.0917 (all data)

[a] $R1 = \sum(|F_o| - |F_c|)/\sum|F_o|$. [b] $wR2 = [\sum(w|F_o^2 - F_c^2|)/\sum w|F_o^2|^2]^{1/2}$.

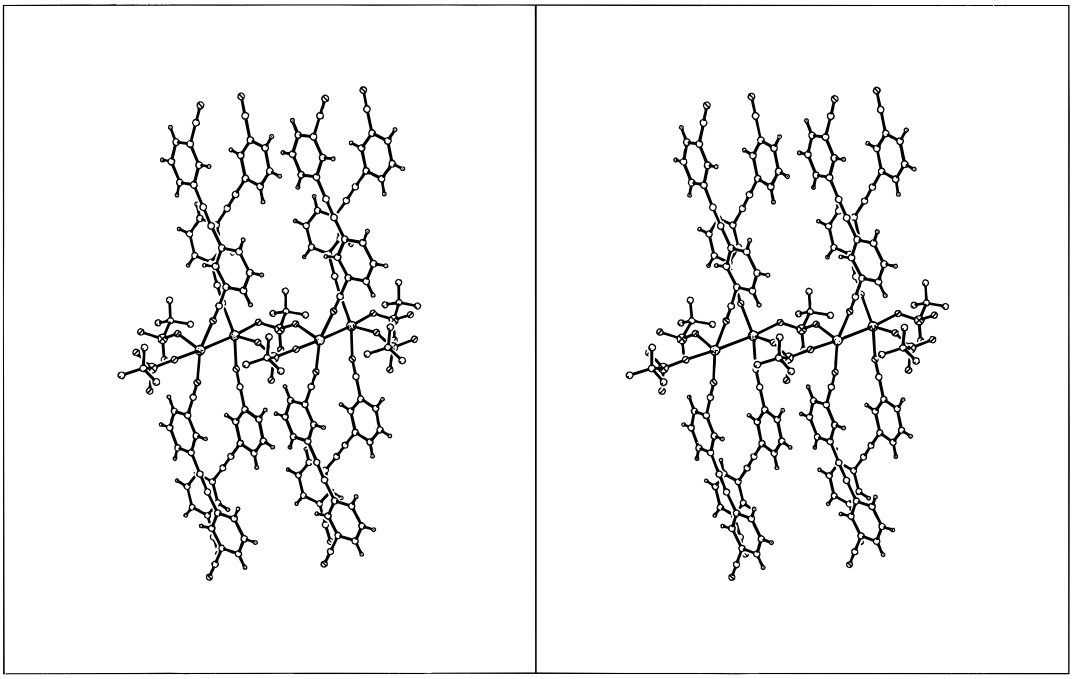

Figure 1. Stereoview of bridged strands from the infinite network [Ag(**1**)CF_3SO_3]C_6H_6 (**2**). 3,3′-DCPA coordinates to silver(I) in the *transoid* conformation. Silver(I) is five-coordinate, bonding to two ligand nitrogen atoms, two counterion oxygen atoms, and a neighboring silver(I) ion. The Ag···Ag separation is 3.377(1) Å. $\pi-\pi$ stacking of 3,3′-DCPA is observed at a face-to-face distance of 3.38 Å. Pairs of strands are bridged by triflate counterions to form the extended sheet topology as the Ag···Ag contacts only bridge two strands. Disordered benzene molecules have been omitted for clarity.

arrangement and adjacent strands pack in the manner shown in Figure 1. This orientation of strands does allow one aromatic ring of a 3,3′-DCPA moiety to engage in $\pi-\pi$ stacking with a ring of another at a face-to-face stacking distance of 3.38 Å. Void space created by this packing is filled by two crystallographically distinct types of benzene molecules which are oriented in a face-to-edge manner with 3,3′-DCPA ligands. The 3,3′-DCPA edge-to-benzene ring plane distances are 3.55 and 3.75 Å. Both benzene molecules show disorder by rotation about the inherent 6-fold axis. The first possesses 2-fold symmetry with a major site occupancy of 0.77. The second benzene molecule has inversion symmetry with a major site occupancy of 0.65.

Crystal Structure of 3,3′-DCPA (1) with $AgCF_3SO_3$ from Toluene: [Ag_2(1)$(CF_3SO_3)_2$] (3). To further probe the coordinating propensity of the triflate ion with silver(I), crystals of 3,3′-DCPA and $AgCF_3SO_3$ were grown from toluene. The resulting structure (complex **3**) consists of undulating sheets in which 3,3′-DCPA coordinates to silver(I) in the *transoid* conformation (see Figure 2). The metal−ligand stoichiometry is 2:1, and no solvent is included. Interestingly, silver(I) is six-coordinate in this structure[7,8] although only one nitrogen of 3,3′-DCPA is bound to each metal ion (Figure 2). The remaining five coordination sites are occupied by a neighboring silver(I) ion and four oxygen atoms of bridging triflate counterions (Figure 2). The Ag···Ag separation[9] is 3.310(0) Å, which is slightly shorter than the distance noted in complex **2**. Two bonds to oxygen (Ag−O distances of 2.428(2) and 2.507(2) Å) and the contact to silver(I) are approximately coplanar. A short Ag−O bond (2.403(2) Å) occupies an apical position, and the

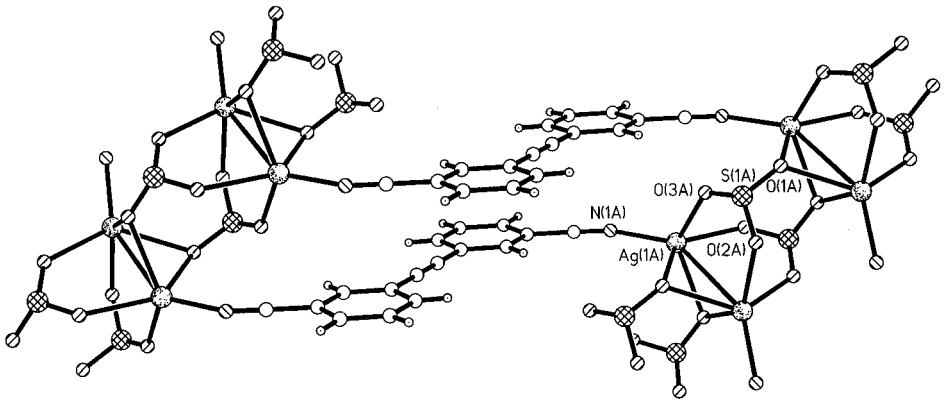

Figure 2. Portion of the infinite, undulating sheet structure $[Ag_2(\mathbf{1})(CF_3SO_3)_2]$ (**3**) crystallized from toluene. Selected atoms are labeled. Trifluoromethyl groups of the triflate ions have been omitted for clarity. As with complex **2**, 3,3′-DCPA coordinates to silver(I) in the *transoid* conformation. Silver(I) is six-coordinate, bonding to one ligand nitrogen atom, four triflate oxygen atoms, and a silver(I) ion. The Ag···Ag separation is 3.310(0) Å. The sheet topology is formed by the extensive bridging of the triflate counterions. A ligand nitrile group overlaps a neighboring ligand aromatic ring at a distance of 3.36 Å. No solvent is incorporated in this structure.

coordination sphere is completed by a long bond to oxygen (2.598(2) Å) and the bond to nitrogen (2.206(2) Å). A C−N−Ag bond angle of 153.0(2)° is observed for this network which is compressed relative to those noted for complex **2** (166.3(3) and 172.3(3)°). This compression shortens the Ag−**1**−Ag distance from 17.01 Å in complex **2** to 15.66 Å in complex **3**. Such a discrepancy given the same ligand and metal ion illustrates the flexible coordination sphere inherent to silver(I).[7]

As was noted for complex **2**, the formation of the two-dimensional network from toluene is mediated by counterion coordination. Although bridging of triflate ions is known,[10] coordination of the three oxygen atoms to four different silver(I) ions is noted in complex **3** and is rather unusual. Despite the uncommon coordination modes of both the silver(I) and triflate ions in this structure, this topology is similar to that of $[Ag_2(4,4'\text{-dicyanodiphenylacetylene})(PO_2F_2)_2]$, which we reported previously.[3] For the structure involving 4,4′-dicyanodiphenylacetylene and $AgPO_2F_2$, undulating sheets result from the bridging of silver(I) ions by the two oxygen atoms of the difluorophosphate species. Also, silver(I) coordinates in a more familiar distorted tetrahedral manner and there are no Ag···Ag contacts. For the 4,4′-dicyanodiphenylacetylene·$AgPO_2F_2$ adduct, we reported that parallel ligands within a sheet engage in face-to-face $\pi-\pi$ stacking as the aromatic rings are in registry laterally. However, in complex **3**, although 3,3′-DCPA molecules are disposed with a usual longitudinal offset, a lateral offset is also noted. As a result, a diagonal offset angle of 43.4° is observed. Therefore, the overlap of aromatic rings is lessened in the present case although there is overlap of a nitrile group with the plane of an aromatic ring at a distance of 3.36 Å.

Crystal Structures of 3,3′-DCPA (1) with $AgPF_6$, $AgAsF_6$, and $AgSbF_6$: $[Ag(\mathbf{1})_2]PF_6$ (4), $[Ag(\mathbf{1})_2]AsF_6$ (5), and $[Ag(\mathbf{1})_2]SbF_6$ (6). The two structures described above both illustrate the affinity of the triflate ion for silver(I). It has been shown by our previous work,[2] and that of others,[11] that employing noncoordinating counterions such as BF_4^-, PF_6^-, AsF_6^-, or SbF_6^- can yield two- or three-dimensional networks through increased ligand coordination (i.e., in lieu of counterion coordination). However, systematic studies involving one ligand and these counterions to probe the effect of counterion size on topology are rare.[2c] With 3,3′-DCPA, crystallization with $AgPF_6$, $AgAsF_6$, and $AgSbF_6$ in ethanol has been performed. The three resulting structures are topologically equivalent, and the metal−ligand stoichiometry is 1:2. For this discussion, all packing parameters have been taken from the 3,3′-DCPA·$AgAsF_6$ adduct (**5**) since atomic positions have been determined most accurately for this structure (as a result of relative crystal quality). The networks in this series are composed of corrugated sheets in which four 3,3′-DCPA molecules coordinate in the *cisoid* conformation to tetrahedral silver(I) ions (see Figure 3). The counterions do not coordinate. Interestingly, in all three structures, three of the four C−N−Ag bond angles about a single silver(I) ion are typical (161.4(3), 165.8(3), and 173.2(3)°); however, the fourth is bent considerably (144.6(3)°).

The *cisoid* conformation of the 3,3′-DCPA ligand restricts the network to two dimensions despite tetrahedral silver(I) coordination. This arrangement, therefore, prevents the formation of a diamondoid network which might have been expected in the presence of a noncoordinating counterion had the ligand adopted the *transoid* conformation (assuming tetrahedral coordination of the metal ion). Therefore, conformational flexibility of 3,3′-DCPA is invoked in order to maximize packing efficiency. For the *cisoid* mode of coordination, the Ag−**1**−Ag distances in complex **5** are 14.10 and 14.91 Å as compared to the aforementioned values of 15.66 and 17.01 Å for the two triflate structures in which 3,3′-DCPA is *transoid*. A portion of the void space created in a single sheet is filled by the interpenetration of a second equivalent network (i.e., a 2-fold interpenetrated structure). Alternatively, this packing may be understood in terms of the intertwining of two 2/1 helices as shown in Figure 4. Each 2/1 helix is derived from a single sheet as shown in the figure. The packing of 2/1 helices envisioned to afford corrugated sheets is made possible by the kinked nature of the *cisoid* ligand conformation. Viewing the interpenetration as arising from the intertwining of helices, while simplifying the analysis, also illustrates the subjective nature of structure interpretation. Also shown in Figure 4 is the accommodation of counterions within this topology.

The helix pitch along the *b*-axis in these structures is 2*b*. As a result, interpenetrated networks are separated by the distance *b* which is 11.930(1) Å in the case of complex **5** (see Table 1). Therefore, parallel ligands of interpenetrated networks do not

(10) Lawrance, G. A. *Chem. Rev.* **1986**, *86*, 17.

(11) See, for example, ref 8 and the following: (a) MacGillivray, L. R.; Subramanian, S.; Zaworotko, M. J. *J. Chem. Soc., Chem. Commun.* **1994**, 1325. (b) Munakata, M.; Wu, L. P.; Yamamoto, M.; Kuroda-Sowa, T.; Maekawa, M. *J. Am. Chem. Soc.* **1996**, *118*, 3117. (c) Hoskins, B. F.; Robson, R. *J. Am. Chem. Soc.* **1990**, *112*, 1546. (d) Carlucci, L.; Ciani, G.; Proserpio, D. M.; Sironi, A. *J. Chem. Soc., Chem. Commun.* **1994**, 2755. (e) Carlucci, L.; Ciani, G.; Proserpio, D. M.; Sironi, A. *J. Am. Chem. Soc.* **1995**, *117*, 4562. (f) Carlucci, L.; Ciani, G.; Proserpio, D. M.; Sironi, A. *Inorg. Chem.* **1995**, *34*, 5698.

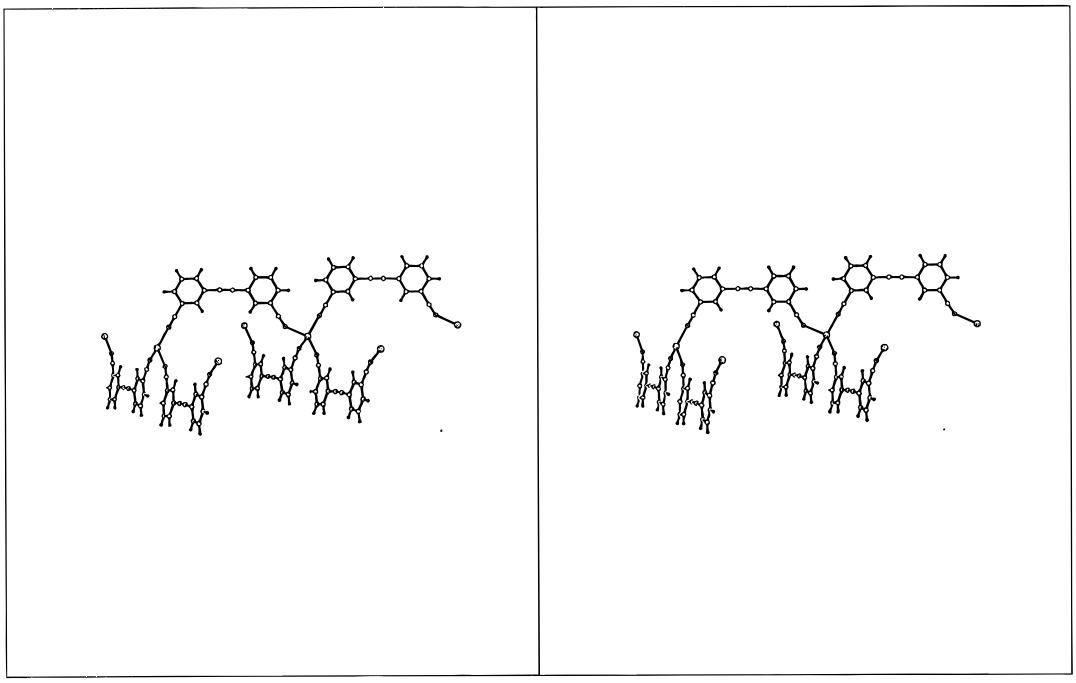

Figure 3. Stereoview highlighting a portion of a single network from the corrugated sheet structure $[Ag(\mathbf{1})_2]AsF_6$ (**5**). Hexafluoroarsenate counterions have been omitted for clarity. This topology is also observed with $AgPF_6$ and $AgSbF_6$ (complexes **4** and **6**, respectively). 3,3′-DCPA coordinates to tetrahedral silver(I) in the *cisoid* conformation. Silver(I) bonds to four ligand nitrogen atoms, and the counterion does not coordinate. For the four-coordinate silver(I) ion shown, the upper left coordinated nitrile group illustrates the unusual C−N−Ag bond angle of 144.6(3)° observed in this structure (similar bond angles are also observed for complexes **4** and **6**). This structure is 2-fold interpenetrated in order to partially fill void space created by a single network (see Figure 4).

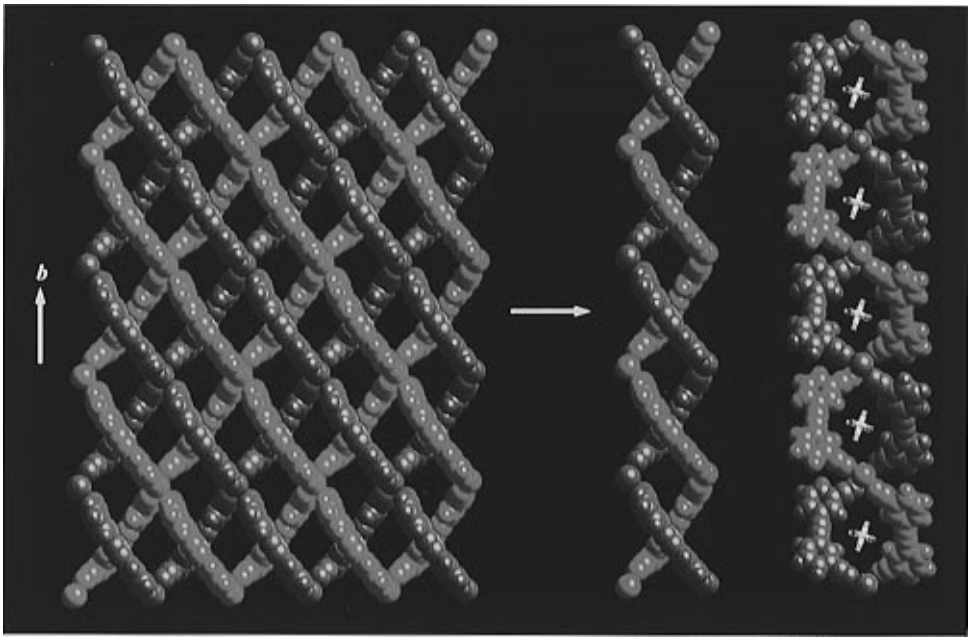

Figure 4. Two intertwined 2/1 helices arising from interpenetration in the corrugated sheet structure $[Ag(\mathbf{1})_2]AsF_6$ (**5**). The helices are derived from the infinite networks as illustrated. The projection on the far right results from an approximate rotation of the middle figure by 90° about the *b*-axis. The inclusion of counterions within this topology is shown on the far right (arsenic is shown in yellow and fluorine is shown in blue). The helix pitch along the *b*-axis is 2*b* and intertwined helices are separated by the distance *b* which is 11.930(1) Å. As a result, $\pi-\pi$ stacking of 3,3′-DCPA does result from interpenetration as the closest face-to-face distance is 6.68 Å. Rather, $\pi-\pi$ stacking is achieved by the interdigitation of networks (see Figure 5).

engage in $\pi-\pi$ stacking, as the shortest plane-to-plane separation is 6.68 Å. $\pi-\pi$ stacking of 3,3′-DCPA is achieved by the interdigitation of a second set of 2-fold interpenetrated sheets (see Figure 5). In this arrangement, the closest face-to-face stacking distance of 3,3′-DCPA is 3.40 Å. This mode of closest-packing may then be viewed as the interdigitation of helices and is only possible if the two sets of interpenetrated sheets are mirror images of one another. Thus, the handedness of 2/1 helices in adjacent, interdigitated sheets is of opposite sense as shown in Figure 6.

In our previous work involving the 9-fold interpenetrated diamondoid networks of 4,4′-biphenyldicarbonitrile and $AgXF_6$ (X = P, As, or Sb),[2c] we observed considerable network deformations as a function of counterion size. However, for the sheet structures presented here, network deformation is minimal in spite of variation of the counterion. Although the

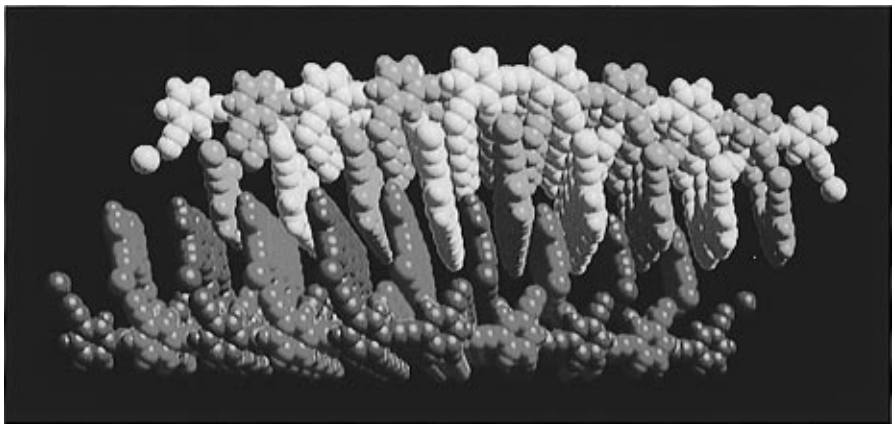

Figure 5. Perspective view of the interdigitation of 2D sheets in $[Ag(\mathbf{1})_2]AsF_6$ (**5**) illustrating $\pi-\pi$ stacking of 3,3′-DCPA. The red and green networks are interpenetrated as are the blue and yellow networks. Interdigitation, therefore, occurs between two sets of interpenetrated sheets. This arrangement allows $\pi-\pi$ stacking of 3,3′-DCPA in a blue-red-yellow-green sequence from left to right. The face-to-face stacking distance is 3.40 Å. Note that the interdigitated portions have been separated from one another vertically for clarity.

Figure 6. Interdigitation in $[Ag(\mathbf{1})_2]AsF_6$ (**5**) in terms of 2/1 helices. The red and green helices are intertwined as are the blue and yellow helices. Interdigitation, therefore, may be viewed as arising between two independent sets of intertwined helices. $\pi-\pi$ Stacking of 3,3′-DCPA is shown in the center of the figure in a yellow-green-blue-red sequence from top to bottom. For the interdigitation of helices to occur, the two independent sets must be of opposite handedness. As can be seen in the figure, the red and green helices propagate counterclockwise and the blue and yellow helices propagate clockwise.

deformations observed in the sheet structures are small, a trend is noted. Comparison of cell constants for the three structures (Table 1) shows that as the size of the counterion decreases (i.e., $SbF_6^- > AsF_6^- > PF_6^-$),[12] the *b*-axis length increases slightly and the *a*- and *c*-axis lengths decrease. In considering th *b*-axis as the 2/1 helix axis as previously discussed, the helix stretches as the counterion size decreases which leads to lateral compressions (along *a* and *c*). These lateral compressions, therefore, alter the dimensions of the counterion channels (Figure 4) in accordance with the size of the included guest. The small deformations that occur for this system are possibly a consequence of the small amount of void space present in a single sheet. It is felt that the void space in a single network is relatively small (as compared to that for a diamondoid network that is interpenetrated by eight other networks, e.g.). For the sheet topology, therefore, allowable network deformation is minimal as unfavorable contacts (and resulting strain on the system) are more readily encountered.[13] Thus, we postulate that the pliability of networks increases with the amount of void space present which is related to the degree of interpenetration.[14]

Crystal Structure of 3,3′-DCPA with $AgClO_4 \cdot H_2O$: $[Ag(\mathbf{1})_2]ClO_4 \cdot H_2O$ (7). In order to further test the generality of the sheet structure to form in the presence of noncoordinating counterions, our study included the use of $AgClO_4 \cdot H_2O$. With this salt, however, a diamondoid network (**7**) results in which *transoid* molecules of 3,3′-DCPA coordinate to tetrahedral silver(I) ions (see Figure 7). The metal−ligand stoichiometry is 1:2. A large amount of void space is created in a single diamondoid framework as the Ag−3,3′-DCPA−Ag distance is 17.02 Å. A majority of this void space is filled through interpenetration resulting in an 8-fold diamondoid network.[15] Remaining space within the lattice is filled by perchlorate ions and water. The counterions and water molecules fill space

(12) Mingos and Rohl have calculated the molecular volumes, V_m, of the PF_6^-, AsF_6^-, and SbF_6^- ions to be 54, 63, and 71 Å^3, respectively. See: (a) Mingos, D. M. P.; Rohl, A. L. *Inorg. Chem.* **1991**, *30*, 3769. (b) Mingos, D. M. P.; Rohl, A. L. *J. Chem. Soc., Dalton Trans*, **1991**, 3419.

(13) It is assumed that, due to symmetry, equivalent deformations take place for each interpenetrated network. Such an observation was made in the diamondoid networks involving 4,4′-biphenyldicarbonitrile and $AgPF_6$, $AgAsF_6$, and $AgSbF_6$.[2c]

(14) Ermer and Lindenberg observed a small deformation in 4-fold interpenetrated diamondoid networks of the dipotassium and disodium salts of 1,2,5,7-adamantanetetracarboxylic acid. The deformation arises from the different packing requirements of the sodium and potassium ions which occupy channels in the two structures. It should be noted that this deformation is less substantial than those observed in the 9-fold diamondoid networks reported in ref 2c. For more on the 4-fold structures, see: Ermer, O.; Lindenberg, L. *Chem. Ber.* **1990**, *123*, 1111.

(15) For other examples of interpenetrated diamondoid networks, see refs 2, 9a, 11a−d, 14, and the following: (a) Ermer, O. *J. Am. Chem. Soc.* **1988**, *110*, 3747. (b) Ermer, O. *Adv. Mater.* **1991**, *3*, 608. (c) Simard, M.; Su, D.; Wuest, J. D. *J. Am. Chem. Soc.* **1991**, *113*, 4696. (d) Wang, X.; Simard, M.; Wuest, J. D. *J. Am. Chem. Soc.* **1994**, *116*, 12119.

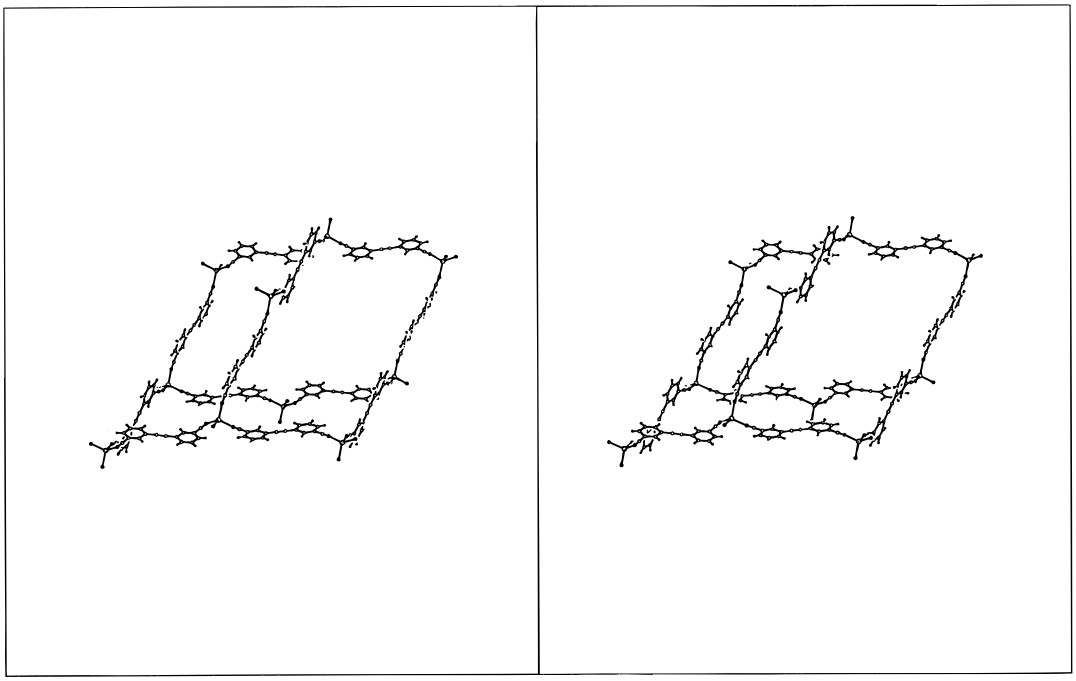

Figure 7. Stereoview of an adamantanoid cage from a single diamondoid network in $[Ag(\mathbf{1})_2]ClO_4 \cdot H_2O$ (**7**). 3,3′-DCPA coordinates in the *transoid* conformation to tetrahedral silver(I) ions. Water molecules and disordered counterions have been omitted for clarity. The structure is 8-fold interpenetrated in order to fill a majority of the void space shown (see Figure 8).

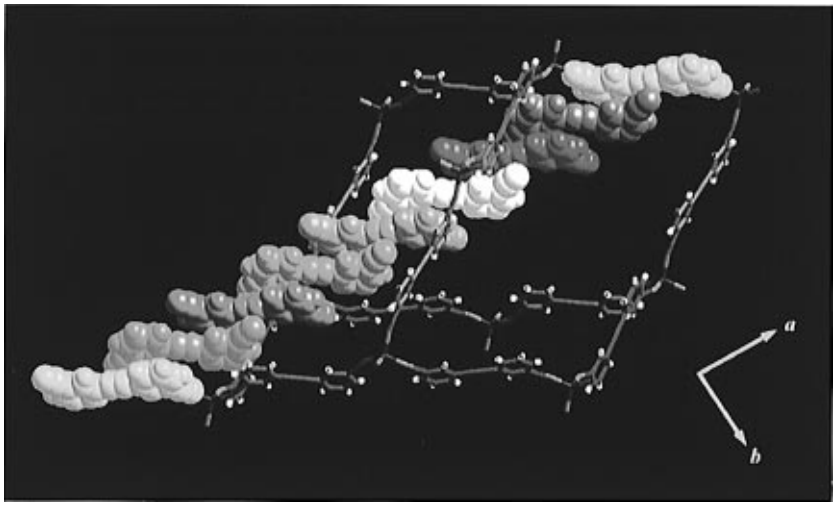

Figure 8. Interpenetration mediated by $\pi-\pi$ stacking in the diamondoid network $[Ag(\mathbf{1})_2]ClO_4 \cdot H_2O$ (**7**). Stacking along the *a*-axis is shown. The face-to-face stacking distance is 3.51 Å. The colors assigned to 3,3′-DCPA molecules in the stack identify ligands derived from independent networks. Thus, the degree of interpenetration is 8.

between networks along the *b*-axis in a $Ag^+-H_2O-ClO_4^--H_2O-Ag^+$ sequence. The packing occurs without counterion channel formation as disordered perchlorate ions are nested between water molecules along *b* and silver(I) ions along *a* and *c* (the Ag···Cl distances are *ca.* *a*/2 and *c*/2; see Table 1). However, channels containing water are visible along the *a*-axis.

Interpenetration in this structure is mediated by $\pi-\pi$ stacking of molecules of 3,3′-DCPA. Face-to-face stacking at a plane-to-plane distance of 3.51 Å occurs along both the *a* and *b* directions. Along *a*, adjacent ligands in the stack are flipped 180° relative to one another such that nitrile groups are not overlayed (see Figure 8). The stacking along *b* is unusual in that a large offset angle causes a 3,3′-DCPA molecule to stack between two fragments each consisting of two halves of 3,3′-DCPA coordinated to silver(I). In order to allow stacking in two directions, mutually perpendicular stacks organize in alternating layers. This type of packing should be contrasted to that which we previously reported for diamondoid networks with 4,4′-biphenyldicarbonitrile.[2] For this system, interpenetration is mediated by $\pi-\pi$ stacking in *one* direction. The π-stacks of 4,4′-biphenyldicarbonitrile ligands form the walls of counterion channels.[2c] For complex **7**, a comparable packing which forms counterion channels likely does not occur due to the inability of the small perchlorate ions[16] to adequately fill space within the expected large channels.[17]

(16) The molecular volume, V_m, of the ClO_4^- ion has been calculated to be 47 Å^3 by Mingos and Rohl. See ref 12.

(17) For diamondoid networks containing counterion channels, it is presumed that the dimensions of the channels will increase as the length of the ligand increases despite interpenetration. As an example, for the 9-fold diamondoid network of 4,4′-biphenyldicarbonitrile with $AgPF_6$,[2] where the Ag−ligand−Ag distance within a network is *ca.* 16.4 Å, a counterion channel *ca.* 6 Å × 10 Å is observed. As a result, the PF_6^- ions are significantly disordered. The notion of forming larger void spaces by increasing the size of framework components was suggested early by Powell. See: Powell, H. M. *J. Chem. Soc.* **1948**, 61.

Conclusions

Novel coordination networks of 3,3′-dicyanodiphenylacetylene (3,3′-DCPA) with silver(I) salts have been prepared and characterized by single-crystal X-ray diffraction. With $AgCF_3SO_3$ in benzene, a sheet structure with included solvent is formed in which silver(I) is five-coordinate. Changing the crystallization solvent to toluene leads to the formation of undulating sheets without solvent incorporation. In this structure, silver(I) adopts an unusual six-coordinate geometry. In both networks involving triflate, 3,3′-DCPA adopts the *transoid* conformation and the bridging of counterions extends the network to two dimensions. With $AgPF_6$, $AgAsF_6$, or $AgSbF_6$, 2-fold interpenetrated sheet structures form in which 3,3′-DCPA coordinates to tetrahedral silver(I) in a *cisoid* fashion. This topology is found to deform only slightly as a function of counterion size which is believed to be a result of the low degree of interpenetration. For these structures, the *cisoid* conformation prevents the formation of a diamondoid network. With $AgClO_4 \cdot H_2O$, however, an 8-fold interpenetrated diamondoid network results through coordination of 3,3′-DCPA in the *transoid* conformation to tetrahedral silver(I). In this case, interpenetration occurs without counterion channel formation. This represents a different mode of packing for interpenetrated diamondoid networks than we reported previously with 4,4′-biphenyldicarbonitrile. The structures resulting from this study, therefore, illustrate how coordination network topology may be influenced significantly by not only the nature of the counterion, but also by the conformation adopted by the ditopic ligand.

Acknowledgment. We thank the School of Chemical Sciences Materials Chemistry Laboratory at the University of Illinois for X-ray data collection. We acknowledge the National Science Foundation (Grant CHE-94-23121) and the U.S. Department of Energy through the Materials Research Laboratory at the University of Illinois at Urbana-Champaign (Grant DEFG02-91-ER45439) for financial support of this work.

Supporting Information Available: Tables of X-ray data for complexes **2**−**7**, including atomic coordinates, displacement parameters, and bond lengths and angles, and a 50% probability thermal ellipsoid plot for each complex (54 pages). Ordering information is given on any current masthead page.

IC970150J